

# Global assimilation of Loon stratospheric balloon observations

L. Coy<sup>1,2</sup>, M. R. Schoeberl<sup>3</sup>, S. Pawson<sup>1</sup>, S. Candido<sup>4</sup>, and R. W. Carver<sup>4</sup>

<sup>1</sup>Global Modeling and Assimilation Office, NASA, GSFC, Greenbelt, MD 20771

<sup>2</sup>SSAI, Lanham, MD 20706

<sup>3</sup>STC, Columbia, MD 21046

<sup>4</sup>Loon, Mountain View, CA 94043

Corresponding author: Lawrence Coy ([lawrence.coy@nasa.gov](mailto:lawrence.coy@nasa.gov))

## Key Points:

- Data-assimilation impact study of stratospheric wind derived from a large number of super-pressure balloons during June-August 2014.
- Assimilated balloon winds can improve local 6-hour wind forecasts in the lower stratosphere based on differences between the balloon's wind and the forecast.
- Balloon wind assimilation can improve wind analyses, especially in the tropics, where results show that tropical waves can be misrepresented with wind errors greater than 10 ms<sup>-1</sup>.

## Abstract

Accurate analyses of stratospheric winds are important for determining realistic constituent transport and providing improved diagnostic studies and forecasts of the stratosphere. This study examines impacts on global meteorological analyses resulting from using winds derived from Loon super-pressure balloons in the lower stratosphere (hereafter Loon winds) as additional input observations to the Goddard Earth Observing System (GEOS) data assimilation system (DAS). To fully investigate the impacts of assimilating the Loon winds, two steps are taken: 1) comparison of the GEOS analysis winds with Loon winds (Control experiment) and 2) examination of the impacts of assimilating the Loon winds into the GEOS DAS (Loon experiment). The time period selected is June-August 2014 when over 150 Loon balloons were launched, mainly in the Southern Hemisphere. In the middle latitudes, the Loon winds and Control winds agree well (Loon balloon zonal wind observation minus forecast, o-f, RMS values of  $\sim 2.75 \text{ ms}^{-1}$ ) and assimilating the Loon winds has a small impact (o-f RMS values unchanged). In the tropics, the Loon observations and Control analysis winds differ more than in middle latitudes (zonal wind o-f RMS  $\sim 3.75 \text{ ms}^{-1}$ ) and assimilating the Loon winds improves the zonal wind o-f RMS by  $\sim 1 \text{ ms}^{-1}$ . In selected cases where the Loon observations and Control analysis differ greatly (o-f RMS values greater than  $10 \text{ ms}^{-1}$ ), assimilating Loon winds significantly decreases the zonal wind o-f RMS by  $5 \text{ ms}^{-1}$ . These decreases in o-f RMS values show that the 6-hour forecasts are improved at the Loon balloon observation locations.

## Plain Language Summary

While satellites routinely measure Earth's global temperatures from space, in-situ wind measurements are relatively scarce, consisting mainly of a network of ground-based weather balloons. Since only a limited number of the weather balloons even reach stratospheric altitudes there is a need for additional stratospheric observations. One option for addition wind information is the use of experimental super-pressure balloons (SPBs). SPBs can remain in the stratosphere for many months traveling with the winds and hence, by reporting their changing positions, providing in-situ wind observations. These SPBs experiments are generally limited in terms of time period and number of balloons. However, over the past few years Loon has been launching hundreds of SPBs (hereafter called Loon balloons) providing a more consistent set of observations of wind in the stratosphere. Here we assimilate some of the Loon balloon winds into the NASA GEOS global data assimilation system (DAS). The DAS combines all observations with an atmospheric model to produce global analysis of winds and temperatures. Results show that including the Loon balloon wind information noticeably effects the global analysis as well as forecasts with the largest impact in the tropics. These results provide direction to future model and analysis improvements.

56

## 57 **1 Introduction**

58       The realistic representation of stratospheric winds is important for understanding the  
59 transport and distribution of trace gases and aerosols needed for seasonal forecasting studies  
60 (Wargan et al., 2018). Routine *in situ* measurement of stratospheric winds, provided by the  
61 relatively sparse radiosonde network yields an incomplete picture of the dynamics of this region.  
62 While extratropical regions analysis wind estimates benefit from the assimilation of satellite-  
63 based radiances via the thermal wind balance, the tropical wind estimates continue to rely on  
64 sparse *in situ* wind measurements, tropospheric cloud track winds, and the atmospheric model's  
65 background wind field. Here we use winds derived from a large number of lower stratospheric  
66 super-pressure balloons (SPBs) as additional input to a global data assimilation system to  
67 examine the potential of these measurements to improve the representation of stratospheric  
68 winds.

69       Data assimilation combines a model (the background forecast) with the observations,  
70 each weighted by their associated errors, to produce a synthesized meteorological analysis.  
71 Global atmospheric data assimilation is routinely used to initialize weather forecasting (Kwon,  
72 2018), produce long term reanalyses (e.g. Gelaro et al., 2017), and assess data impacts (e.g. Privé  
73 et al., 2013). Lower stratospheric winds derived from the limited number of scientific SPB  
74 campaigns have only rarely been used in global atmospheric data assimilation systems. One  
75 study, the assimilation of the Vorcore project SPBs, demonstrated improvements in the  
76 assimilation system forecasts during the Southern Hemisphere spring breakup of the  
77 stratospheric polar vortex (Rabier et al., 2010, their Fig. 9). More commonly, however, SPBs  
78 have been used as independent measurements for assessing the quality of reanalysis products  
79 (e.g., Podglajen et al., 2014; de la Camara et al., 2010). These comparisons can help identify  
80 regions and times where wind uncertainties are largest and identify dynamical wave systems that  
81 may be unresolved by the data assimilation system.

82       Loon (described below) has launched a large number of SPBs as part of their goal to  
83 provide internet service to underserved regions. These balloons have minimal atmospheric  
84 instrumentation (Friedrich et al., 2016), but their motion provides important information on  
85 ambient wind fields. Here we add the Loon balloon winds to a data assimilation system (DAS) to  
86 determine their impact. More specifically, we assimilate the Loon winds and look for possible  
87 improvements in short term (6 hr) forecasts and wind analysis in a global DAS. Similar to the  
88 time period examined in Friedrich et al. (2016), we have chosen June-August 2014. During this  
89 period, there were over 150 Southern Hemisphere (SH) launches along with several tropical  
90 launches. We use these Loon balloon derived wind observations to evaluate their potential for  
91 supplementing the current data assimilation observation set and to identify potential  
92 discrepancies between current data assimilation winds, the forecasted winds, and the Loon  
93 observations.

94       The plan of this paper is as follows: Section 2 describes the Loon observations followed  
95 by a description of the data assimilation system and the experiments run, Section 3 presents the  
96 results of the experiments, and Section 4 provides the conclusions.

## 2 Loon observations and MERRA-2 system description

### 2.1 Loon Observations

The Loon program is designed to use stratospheric balloons to provide internet connectivity to people in unserved or underserved areas. These balloons are tracked by the Global Positioning System (GPS), and their accurate trajectories (recorded approximately every one to three minutes) can be used to derive local winds. The balloons are typically located at altitudes between 100 and 30 hPa. The pressure altitude typically changes over the duration of a balloon flight as the Loon balloons have the ability to execute a controlled change in altitude that is used to adjust the balloon's trajectory in regions with vertical wind shear. Balloons are assumed to be carried with the ambient flow on the horizontal and thus the horizontal winds can be estimated from changes in position. Loon winds were calculated from the balloon positions using a 3-point Lagrangian differencing scheme to account for uneven spacing with time. Friedrich et al. (2016) note that the GPS observations have an uncertainty of 10 m, which translates to an uncertainty of up to 20 m over one minute, leading to an uncertainty in the derived winds of less than one meter per second ( $0.67 \text{ m s}^{-1}$ ). Note, that there is also uncertainty arising from SPBs not being perfect tracers, that is, the balloons have some inertia and may underrepresent rapid wind changes. The pressure sensor accuracy is 1.5 hPa, which provides a small uncertainty in the altitude of the Loon balloons. This altitude uncertainty ( $\sim 200\text{m}$  at 50 hPa) is smaller than the vertical data assimilation grid ( $\sim 1.2 \text{ km}$ ) in the lower stratosphere. Loon balloons also provide temperature observations, which Friedrich et al. (2016) found had significant biases compared to a number of reanalyses including MERRA-2 and thus are not used in our assimilation. The Loon gravity wave spectra from this same data set were examined in Schoeberl et al. (2017) and the amplitudes and spectral slopes were found to be consistent with past SPB observations (Boccara et al., 2008; Hertzog et al., 2008; Podglajen et al., 2016).

### 2.2 The GEOS Data Assimilation System: MERRA-2 Configuration

The Modern-Era Retrospective analysis for Research and Applications, Version-2 (MERRA-2) reanalysis extends from 1980 to the present (Gelaro et al., 2017; Bosilovich et al., 2015). It uses a fixed version of the Goddard Earth Observing System (GEOS) data assimilation system, with a horizontal resolution of about 50km. The GEOS model (e.g., Molod et al., 2015) uses a cubed-sphere grid in a C180L72 configuration: each face of the cube nests a  $180 \times 180$  grid with 72 layers, extending from the surface to 0.01 hPa. In the lower stratosphere, the vertical level spacing is close to 1 km.

For this study, the MERRA-2 configuration of the GEOS DAS was run twice. A control experiment (Control) used the standard MERRA-2 observations described in McCarty et al. (2016). The second experiment (Loon) additionally assimilated the Loon winds. The control experiment provides the baseline difference between the Loon winds and the DAS winds as well as the DAS short (6 hr) background forecast. The second experiment includes the impact of the Loon winds on both the DAS and the forecast. Both experiments were initialized on 31 May 2014 21 UTC and run continuously until 31 August 2014 21 UTC.

The three-dimensional variational (3D-Var) GEOS DAS used in MERRA-2 performs a global analysis every six hours based on observations spanning the six-hour data window centered at

the analysis time. A six-hour forecast initialized with the analysis then provides a first-guess (background) field at for the next analysis cycle. The full MERRA-2 suite of input data for June-August 2014 was used in the Control experiment, including conventional observations (e.g. radiosondes, aircraft observations, ground based radars, wind profilers), and satellite-derived estimates of wind (e.g. cloud-tracked winds, scatterometers) and temperature (e.g. radiances, GPSRO-Global Positioning System Radio Occultation) as described in McCarty et al. (2016). The Control experiment results differ slightly from the MERRA-2 results because a minor bug fix in the data selection process occurred after the MERRA-2 2014 runs were completed. In addition, to simplify the experimental set up, the Control experiment was run without the MERRA-2 aerosol assimilation component. Use will be made of this difference between the Control experiment and MERRA-2 to help isolate the effects of the Loon assimilation.

For the Loon experiment, the Loon winds were added to the MERRA-2 observation suite and treated as additional radiosonde wind measurements in terms of observations error specification. All the Loon wind data was used in this study with no thinning. The DAS weights the observations based on an observation error value relative to a model background forecast error value. The 3D-Var MERRA-2 DAS uses time-independent values of the observation error and model error derived from DAS tuning experiments. The MERRA-2 DAS radiosonde wind observation errors vary in altitude but are uncorrelated. In the lower stratosphere the radiosonde wind observation errors are  $\sim 3 \text{ ms}^{-1}$ . This is larger than the estimate of the Loon winds stated above, however this value includes an estimate of the error of representing a DAS grid box by a single point observation. The MERRA-2 DAS background error values were estimated using the forecast method of Wu et al. (2002). This procedure generates the background wind error and covariances directly in terms the model stream function and velocity potential variables along with their associated horizontal and vertical length scales. In terms of wind speed, dividing the stream function by the horizontal scale yields a value of  $\sim 3 \text{ ms}^{-1}$  in the tropical lower stratosphere, similar to the DAS observation error. These model error quantities vary with latitude as well as with altitude. The final assimilation perturbation and spatial spreading of the Loon observation by the MERRA-2 DAS can be seen in the results (Fig. 3) to be discussed below.

The distribution of the Loon observations during June-August 2014 is shown in Fig. 1. Figure 1a sums the number of Loon balloon wind observations at altitudes above 100 hPa in latitude and longitude. Most of the balloons were launched from New Zealand and remained in the middle latitudes of the SH where they tend to circle the globe. In addition, there were five launches from Brazil ( $43^\circ\text{W}$ ,  $5^\circ\text{S}$ ) with durations greater than 9 days that will be examined in detail below. The distribution in altitude (Fig. 1b) shows observation density peaks at approximately 65 and 55 hPa. These two peaks in the vertical are created as the balloons are adjusted in altitude during flight. Most of the SH observations are at pressures higher than 50 hPa. There are typically 8-20 balloons reporting during each 6-hour assimilation cycle.

Figure 2a shows several sample Loon balloon trajectories during June 2014. These were launched from Brazil near  $5^\circ\text{S}$  and show consistent North/South oscillations about the Equator. These are likely a signature of mixed Rossby-gravity waves (Vial et al., 2001; Podglajen et al., 2014). Figure 2b shows all the Loon balloon trajectories during a 6-hour data assimilation window in mid-August when the number of Loon balloons was large. Note that the balloons provide wind information over the oceans where radiosonde measurements are sparse. At each

analysis time, wind observations derived from these trajectories are incorporated into the DAS for our experiment.

The assimilation system distributes the Loon information over the spatial domain. By interpolating the assimilated and forecasted winds from the Control experiment to the Loon balloon locations, it was possible to compute the differences in this system compared to the Loon winds. Differencing these output fields from the Control and Loon experiments highlights the impacts of the Loon winds on the global assimilation.

### 3 Results

The Loon and Control experiments were both initialized so that the first analysis cycle was for 1 June 00 UTC 2014. The DAS incorporated the Loon data at all levels (troposphere and stratosphere) as the data became available. The direct impact of the Loon winds was found between 50—70 hPa where the Loon provided most of their observations (Fig. 1b).

The difference between the new analysis and the “first-guess” (or background forecast) is called the increment and highlights the changes to the forecast created by the DAS from the observations. While the increment fields are influenced by all the observations, the impact of the Loon winds on the assimilation can be gauged by examining the difference in the increments from the Control and Loon runs. As an example of the spreading of the Loon balloon information by the DAS, Fig. 3 shows the increment differences that result from assimilating the Loon observations for a single analysis time (20 June 2014 00 UTC). As expected, all of the increment differences appear to be collocated with balloon locations. In Fig. 3a, the largest increment difference is located near southern India, close to a Loon location. At this location, the zonal wind differences show a dipole pattern with magnitude of approximately  $4 \text{ ms}^{-1}$ . This dipole pattern shows that the analysis is spreading the Loon observation in the horizontal vorticity field. The Loon observations produce wind increment differences that extend about  $\pm 5^\circ$  from the balloon location. Smaller magnitude increments occur near other Loon locations because the Loon winds are close to the actual wind forecasts or not located exactly in the selected cross section.

Figure 3b shows pressure versus longitude zonal and meridional wind increments along the equator. The largest wind increment differences are co-located with Loon measurements near India. These are the highest altitude ( $\sim 50 \text{ hPa}$ ) wind increments in Fig. 3b, but there are smaller wind differences at  $\sim 70 \text{ hPa}$  near  $45^\circ\text{E}$  associated with the Loon observations above. We find that the wind increment differences extend vertically approximately  $\pm 1 \text{ km}$  about the balloon observations. The meridional wind differences (not shown) are similar in magnitude and structure to the zonal wind increments. In this example, the direct assimilation response to the Loon observations is confined mainly to the 100–30 hPa altitude region. As discussed in Section 2.2., the vertical and horizontal scales of this spreading of the Loon observations is determined by the model error stream function and velocity potential horizontal and vertical scales set by the DAS.

Figure 3 also shows differences in the zonal wind increments below the tropopause. These tropospheric increment differences grow over time from the initial start (about 20 days earlier in this example) and ultimately cause the two assimilation analyses to diverge, even in regions far

from the Loon observation locations. Figure 4 shows the zonal RMS difference of the zonal wind component between the Loon and Control assimilations as a function of time at two levels. In the lower stratosphere, Fig. 4a, the Loon winds are assimilated in June mainly in the tropics and as a result the largest differences are found near the equator. During July and August most of the Loon balloons are being launched in the southern mid-latitudes and this region shows more differences between the Loon and Control run during those times. Differences are seen in the upper troposphere (Fig. 4b) that are not directly associated with the pattern of the Loon balloon coverage. These result from the differences in small scale features (not shown), associated with sub-grid parameterized convection (not directly constrained by the DAS) that accumulate over time in the two systems. This is demonstrated in Fig. 5, where the Control is compared to MERRA-2 (GMAO, 2015), systems that differ only slightly in their configuration as described in Section 2.2. Figure 5a shows some tropical differences, but not the same pattern as in the Loon experiment (Fig. 4a), while Fig. 5b, in the upper troposphere, shows a similar difference pattern to that depicted in Fig. 4b. This represents a random background difference, a measure of data assimilation uncertainty, between two nearly identical DAS experiments.

Figure 6 summarizes the zonal wind RMS differences between the Loon and the Control for June and August 2014 that are created solely by adding the Loon information (after subtracting the background difference described above). In June (Fig 6a) the changes are mainly evident in the tropics and influence the tropical lower stratospheric winds, while in August (Fig. 6b) the mid-latitude Loon balloon influence the mid-latitude lower stratospheric winds and upper troposphere to about 200 hPa. The RMS differences peak at  $\sim 0.5 \text{ ms}^{-1}$  in June and  $\sim 1.5 \text{ ms}^{-1}$  in August. Note that these zonal mean RMS values, taken from the globally gridded analyses, depend on the distribution of the Loon balloons in longitude and time as well as the Loon induced changes to the analysis. During June the number of Loon balloons is relatively small, available only in the second half of the month, and the tropical Loon balloons cover only a limited range of longitudes, resulting in relatively small zonal mean RMS values. However, during August the relatively large number of SH middle latitude Loon balloons consistently cover most longitudes, resulting in relatively large zonal mean RMS values.

Along with the global increment fields the DAS interpolates the global forecasted winds to the observation locations. The difference between the observations and the background forecast (o-f) at the observation locations yields the increment values (also known as “innovations” or “departures”) for each observation. Smaller o-f increment values denote a better model forecast based on improved initial conditions at the last analysis time. The RMS (root mean square) of the averaged o-f increment values for the three-month experiment time period are shown in Fig. 7 as a way of summarizing the Control and Loon experiments. The o-f increment values are averaged in three latitude bands, southern hemisphere, equatorial region, and northern hemisphere. Figure 7a, the zonal wind RMS, shows that the two experiments have similar values outside of the equatorial region; however, the Loon experiment RMS value is  $\sim 1 \text{ ms}^{-1}$  smaller than the control in the equatorial region. The forecast improvement using the Loon balloons is more apparent in Fig. 7b, where zonal wind increments are averaged only when the control zonal wind o-f increments are greater than  $10 \text{ ms}^{-1}$ . In the tropics these large control zonal wind increments occurred during 2.2% of the observations. In this case the tropical Loon winds improve the RMS values by  $\sim 6 \text{ ms}^{-1}$ , showing that, when the control assimilation is far from the Loon observations, assimilating the Loon winds can greatly reduce the DAS o-f increments. Similar results hold for the meridional wind RMS (Fig. 7c and d). The tropical

meridional wind forecast improvement is relatively small when all the observations are considered ( $\sim 0.3 \text{ ms}^{-1}$ ; Fig. 6c); however, as with the zonal wind, when only observations with control meridional wind increments greater than  $10 \text{ ms}^{-1}$  are included (Fig. 6d) the RMS is  $\sim 4 \text{ ms}^{-1}$  less than the control experiment RMS values. In summary, the RMS results show that the wind forecasts, and by inference, the initial time analyses, are mainly improved in the tropics when the Loon winds are included in the DAS. An example Loon balloon trajectory that includes zonal wind o-f values greater than  $10 \text{ ms}^{-1}$  is shown below (Fig. 10a).

Figure 8 examines the potential influence of the Loon observations on other tropical observations in the assimilation system in terms of their respective O-F RMS values for the 14-26 June 2014 time period when the Loon observations were found in the tropics. While the Loon assimilation improves over the control by  $\sim 1 \text{ ms}^{-1}$  with respect to the Loon observations at the Loon locations, the RMS o-f values for radiosonde winds and temperatures along with the GPSRO bending angles are little changed. This indicates that the assimilated Loon observations are mainly influencing the assimilation locally, near the Loon locations.

As specific example of the tropical improvements, the trajectory of one of the Loon balloons launched from Brazil is examined in detail (Figs. 9 and 10). Figure 9 shows the analysis winds sampled along the balloon trajectory for the control experiment (Fig. 9a) and the Loon experiment (Fig. 9b) over 7-21 June 2014. The balloon trajectory is plotted over the wind vectors with numbers denoting the 00 UTC location on the indicated date. The trajectory altitude was generally above 54 hPa (red trajectory) except for near 10 June when the Loon altitude was adjusted to a lower level near 64 hPa (blue trajectory). The winds in the control experiment (Fig. 9a) are often unaligned with the trajectory, an indication of poor agreement with the balloon's trajectory. This is especially apparent on 9, 12, 20 June. In contrast, the Loon experiment (Fig. 9b) shows good alignment between the wind arrows and the trajectory. The reader may note that June 13 is not shown. On this date the DAS failed to converge as a result multiple Loon balloons being within the same assimilation grid box at that time providing conflicting information (e.g. the presence of unresolved short wavelength gravity waves).

These results from Fig. 9 are displayed quantitatively in Fig. 10, where the zonal (Fig. 10a) and meridional (Fig. 10b) wind components are plotted as a function of time for the same trajectory in Fig. 9. This Loon balloon track provides an example of zonal wind o-f values greater than  $10 \text{ ms}^{-1}$ . The Loon experiment (red) agrees well with the Loon balloon observations (black), while the control experiment (blue) often differs significantly from the observations, especially near the end of the Loon balloon trajectory (19-21 June). This is also shown by comparing the red and blue daily o-f increment RMS values calculated for the Loon and control experiments respectively (Fig. 10). The Loon experiments o-f increment RMS (red) are always smaller than the Control o-f increment RMS (blue). The source of these differences between the Loon and Control experiment are still being investigated but the change in the Loon balloon altitude from 9 to 10 June 2014 (shown as the change from red to blue color trajectory in Fig. 9) and the subsequent better agreement for the Control experiment with the Loon observations in Fig. 10a suggests that the vertical shear in Control analysis is sometimes mis-located in altitude.

Figure 11 shows the tropical vector wind field and relative vorticity at 52 hPa on 19 June 2014, 12 UTC, a time when the Loon experiment differed greatly from the Control (Fig. 10). At this time the Loon experiment (Fig. 11a) shows are stronger region of anticyclonic relative vorticity



at the equator and 75°E than the Control experiments (Fig. 11b) with associated strong southward flow near 80°E (Fig. 11c). The largest changes created by the Loon observations remain in the vicinity of the three Loon balloons being assimilated in the tropics at this time (Fig. 11c). These differences found between the Loon and Control analyses are similar in magnitude and structure to those found between analyses and long-duration balloon flights in early 2010 by Podglajen et al. (2014) and attributed to the misrepresentation of lower stratospheric tropical waves in the analyses. The wave pattern in Fig. 11 reflects the structure of a mixed Rossby-gravity wave and as noted in Podglajen et al. (2014), these waves can have small-scale vertical structures that may be difficult to represent given the current DAS vertical resolution. Figure 10a gives some evidence of this sensitivity to analysis vertical wind shear as it shows that the Control experiment agrees better with the Loon balloon observations after 10 June 2014 when the altitude of the Loon balloon is adjusted from 54 to 64 hPa.

#### 4. Conclusions

In summary, the Loon winds have been successfully assimilated into the MERRA-2 configuration of the GEOS DAS. The DAS treated the winds derived from the balloon positions in the same manner as additional radiosonde winds and their inclusion in a full three-dimensional assimilation system allows for their impacts over deep layers and on other fields (such as temperature). To quantitatively determine the impact of Loon wind assimilation we performed, the two GEOS DAS runs one with (Loon) and one without (Control) assimilating the Loon data. The improvements to the forecast (Fig. 7) as well as the drawing of the analysis to the balloon observations (Fig. 10) shows the impact. Assimilating these lower stratospheric Loon observations led to only a small change on the middle latitude forecast skill, indicated by the small decrease in RMS (Fig. 7b and d) of the wind o-f increment. However, the impacts of Loon winds on tropical regions were much more substantial, showing significant improvements in forecast skill, especially in situations when the analyzed winds in the control experiment were far from the Loon observations.

As noted in Section 3, the wind fields in the Control and Loon experiments diverged with time, leading to significant wind differences. This is illustrated in the RMS of the analysis wind differences between the Loon and the Control experiments for June and August 2014 (Fig. 6). While the Loon effects are concentrated mainly in the lower stratospheric at balloon float altitudes, there are hints that the troposphere is being influenced by the Loon balloons as well. For example, the 0.25 ms<sup>-1</sup> contour in Fig. 6b extends down to 700 hPa between -60 and -50°S. There is also the possibility that the assimilated Loon winds can influence the longer seasonal mean stratospheric circulation. We plan to conduct further investigations of these issues.

The ongoing Loon balloon flights provide a substantial data set for increasing understanding of the dynamics of the lower stratosphere (Friedrich et al., 2016; Podglajen et al., 2014; Schoeberl et al., 2017). This study shows that the enhancement of the standard observing system used in meteorological reanalyses with the Loon balloon data can have a significant impact on the quality of the assimilated fields in the lower stratosphere. In particular, this study has shown that the tropical Loon observations can effectively augment the sparse radiosonde wind observations, leading directly to improvements in the assimilated wind fields in the lower stratosphere. Given the beneficial impacts of the Loon wind data on analyses in the tropical lower stratosphere, future work will investigate impacts of this new observation type over longer

354 periods (the ongoing Loon balloon observations began in 2013) with a view towards using them  
355 in future GEOS reanalyses and forecasts. Impacts on trace-gas transport in the tropics, including  
356 troposphere-stratosphere exchange and on the sub-seasonal to seasonal prediction of tropical-  
357 extratropical teleconnections will also be the subject of future studies with the GEOS system.  
358 Additionally, this work may have relevance to the effects of assimilating lower stratospheric  
359 winds obtained by satellite systems such as the recently launched ADM Aeolus mission  
360 (Reitebuch et al., 2009).

## Acknowledgments

This research was performed with funding from the NASA Modeling, Analysis and Prediction program. Resources supporting this work were provided by the NASA High-End Computing (HEC) Program through the NASA Center for Climate Simulation (NCCS) at Goddard Space Flight Center. Loon balloon data are available from Loon. The data assimilation code, and model output used in this research are archived and available from the NASA Global Modeling and Assimilation office. We would like to thank Meta Sienkiewicz of the NASA Global Modeling and Assimilation Office for providing the code to ready the Loon observations for assimilation. We would also like to thank the anonymous reviewers for their insightful and helpful comments.

## References

- Boccara, G., Hertzog, A., Vincent, R. A., & Vial, F. (2008), Estimation of gravity-wave momentum fluxes and phase speeds from quasi-Lagrangian stratospheric balloon flights. 1: Theory and simulations, *J. Atmos. Sci.*, 65, 3042-3055.
- Bosilovich, M. G., Akella, S., Coy, L., Cullather, R., Draper, C., Gelaro, et al. (2015). MERRA-2: Initial Evaluation of the Climate. NASA Tech. Rep. Series on Global Modeling and Data Assimilation, *NASA/TM-2015-104606*, Vol. 43, 139 pp.
- de la Camara, A., Mechoso, C. R., Ide, K., Walterscheid, R., & Schubert, G. (2010). Polar night vortex breakdown and large-scale stirring in the southern stratosphere. *Clim. Dyn.*, 35, 965-975. <https://doi.org/10.1007/s00382-009-0632-6>
- Friedrich, L. S., McDonald, A. J., Bodeker, G. E., Cooper, K. E., Lewis, J., & Paterson, A. J. (2017). A comparison of Loon balloon observations and stratospheric reanalysis products. *Atmos. Chem. Phys.*, 17, 855-866. <https://doi.org/10.5194/acp-17-855-2017>
- Gelaro, R., McCarty, W., Suarez, M. J., Todling, R., Molod, A. M., Takacs, et al. (2017). The Modern-Era Retrospective Analysis for Research and Applications, Version-2 (MERRA-2). *J. Climate*, 30, 5419-5454. <https://doi.org/10.1175/JCLI-D-16-0758.1>
- Global Modeling and Assimilation Office (GMAO) (2015). MERRA-2 inst3\_3d\_asm\_Nv: 3d,3-Hourly,Instantaneous,Model-Level,Assimilation,Assimilated Meteorological Fields V5.12.4, Greenbelt, MD, USA, Goddard Earth Sciences Data and Information Services Center (GES DISC), Accessed: 15 June 2018, [10.5067/WWQSQ8IVFW8](https://doi.org/10.5067/WWQSQ8IVFW8)
- Hertzog, A., Boccara, G., Vincent, R. A., Vial, F., & Cocquerez, P. (2008) Estimation of gravity-wave momentum fluxes and phase speeds from quasi-Lagrangian stratospheric balloon flights. Results from the Vorcore campaign in Antarctica, *J. Atmos. Sci.*, 65, 3056-3070.
- Kwon, I., S. English, W. Bell, R. Potthast, A. Collard, & B. Ruston (2018). [Assessment of Progress and Status of Data Assimilation in Numerical Weather Prediction](https://doi.org/10.1175/BAMS-D-17-0266.1). *Bull. Amer. Meteor. Soc.*, 99, ES75–ES79, <https://doi.org/10.1175/BAMS-D-17-0266.1>
- McCarty, W., Coy, L., Gelaro, R., Huang, A., Merkova, D., Smith, E. B., et al. (2016), MERRA-2 Input Observations: Summary and Assessment. NASA Technical Report Series on Global Modeling and Data Assimilation, *NASA/TM-2016-104606*, Vol. 46, 61 pp.
- Molod, A., Takacs, L., Suarez, M., & Bacmeister, J. (2015). Development of the GEOS-5 atmospheric general circulation model: Evolution from MERRA to MERRA-2. *Geosci. Model Dev.*, 8, 1339–1356. <https://doi.org/10.5194/gmd-8-1339-2015>
- Podglajen, A., Hertzog, A., Plougonven, R., & Žagar, N. (2014). Assessment of the accuracy of (re)analyses in the equatorial lower stratosphere, *J. Geophys. Res. Atmos.*, 119, 11,166–11,188. <https://doi.org/10.1002/2014JD021849>
- Podglajen, A., Hertzog, Plougonven, A. R., & Legras, B. (2016). Lagrangian temperature and vertical velocity fluctuations due to gravity waves in the lower stratosphere, *Geophys. Res. Lett.*, 43, 3543-3553.
- Privé, N. C., R. M. Errico, and K.-S. Tai (2013). The influence of observation errors on analysis error and forecast skill investigated with an observing system simulation experiment, *J. Geophys. Res. Atmos.*, 118, 5332–5346, doi: 10.1002/jgrd.50452.

- Rabier, F., Bouchard, A., Brun, E., Doerenbecher, A., Guedj, S., Guidard, V., Karbou, F., Peuch, V.-H., El Amraoui, L., Puech, D., et al. (2010). The CONCORDIASI project in Antarctica, *B. Am. Meteorol. Soc.*, 91, 69–86, <https://doi.org/10.1175/2009BAMS2764.1>
- Reitebuch, O., Lemmerz, C., Nagel, E., Paffrath, U., Durand, Y., Endemann, M., Fabre, F., & Chaloupy, M. (2009). [The Airborne Demonstrator for the Direct-Detection Doppler Wind Lidar ALADIN on ADM-Aeolus. Part I: Instrument Design and Comparison to Satellite Instrument.](https://doi.org/10.1175/2009JTECHA1309.1) *J. Atmos. Oceanic Technol.*, 26, 2501–2515, <https://doi.org/10.1175/2009JTECHA1309.1>
- Rienecker, M. M., Suarez, M. J., Gelaro, R., Todling, R., Bacmeister, J., Liu, E., et al. (2011). MERRA: NASA's Modern-Era Retrospective Analysis for Research and Applications. *J. Climate*, 24, 3624–3648. <https://doi.org/10.1175/JCLI-D-11-00015.1>
- Schoeberl, M. R., Jensen, E., Podglajen, A., Coy, L., Lodha, C., Candido, S., & Carver, R. (2017). Gravity wave spectra in the lower stratosphere diagnosed from project loon balloon trajectories, *J. Geophys. Res. Atmos.*, 122, 8517–8524. <https://doi.org/10.1002/2017JD026471>
- Vial, F., Hertzog, A., Mechoso, C. R., Basdevant, C., Cocquerez, P., Dubourg, V., & Nouel, F. (2001). A study of the dynamics of the equatorial lower stratosphere by use of ultra-long duration balloons; 1. Planetary scales, *J. Geophys. Res.*, 106, 22725–22743.
- Wargan, K., Orbe, C., Pawson, S., Ziemke, J. R., Oman, L. D., Olsen, M. A., et al. (2018). Recent decline in extratropical lower stratospheric ozone attributed to circulation changes. *Geophysical Research Letters*, 45, 5166–5176. <https://doi.org/10.1029/2018GL077406>
- Wu, W., R.J. Purser, and D.F. Parrish (2002): [Three-Dimensional Variational Analysis with Spatially Inhomogeneous Covariances.](https://doi.org/10.1175/1520-0493(2002)130<2905:TDVAWS>2.0.CO;2) *Mon. Wea. Rev.*, 130, 2905–2916, [https://doi.org/10.1175/1520-0493\(2002\)130<2905:TDVAWS>2.0.CO;2](https://doi.org/10.1175/1520-0493(2002)130<2905:TDVAWS>2.0.CO;2)

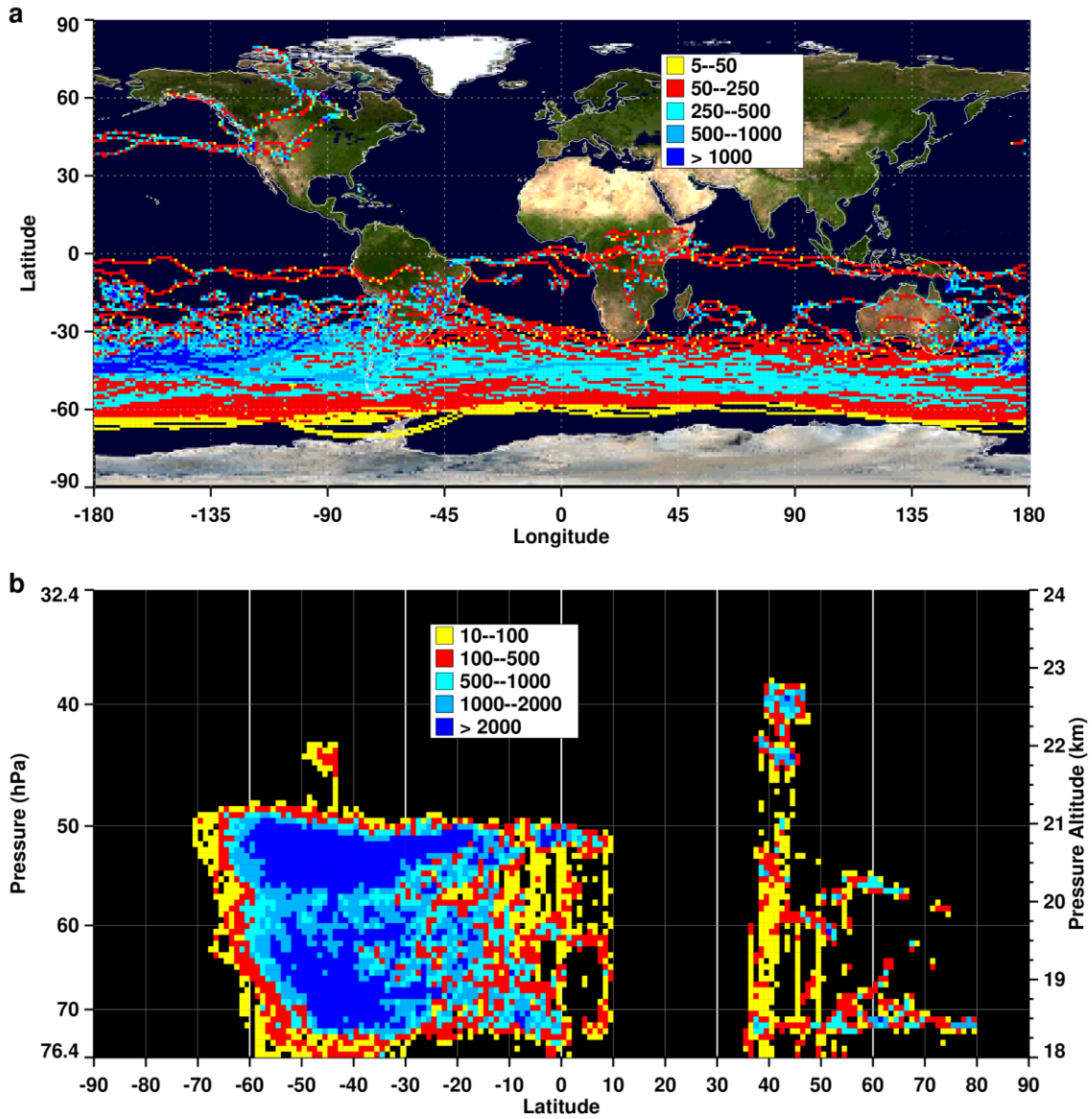


**Figure 1:** Number of Loon observations available during June-August 2014 as a function of: a) latitude and longitude ( $1^\circ \times 1^\circ$  grid box size, pressure less than 100 hPa) and b) latitude and pressure altitude ( $1^\circ \times 75\text{m}$  grid box size). The color scales reflect the density of observations.

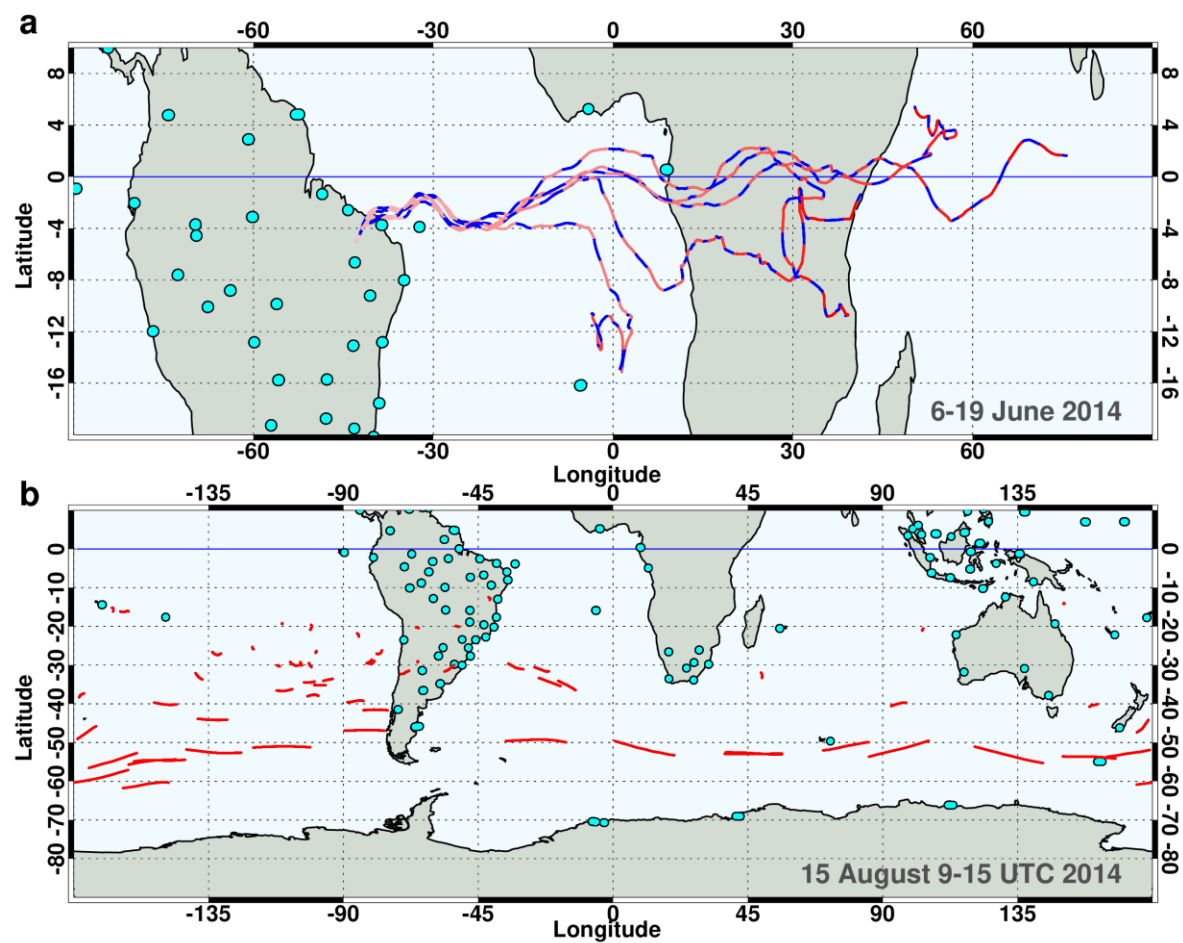


**Figure 2:** a) Sample trajectories 6—19 June 2014 and b) 15 August 9-15 UTC 2014. Alternating blue and red colors in a) denote six-hour intervals. The cyan circles denote radiosonde observations above 70 hPa for a) 12 June 2014 12 UTC and b) 15 August 12 2014 UTC.

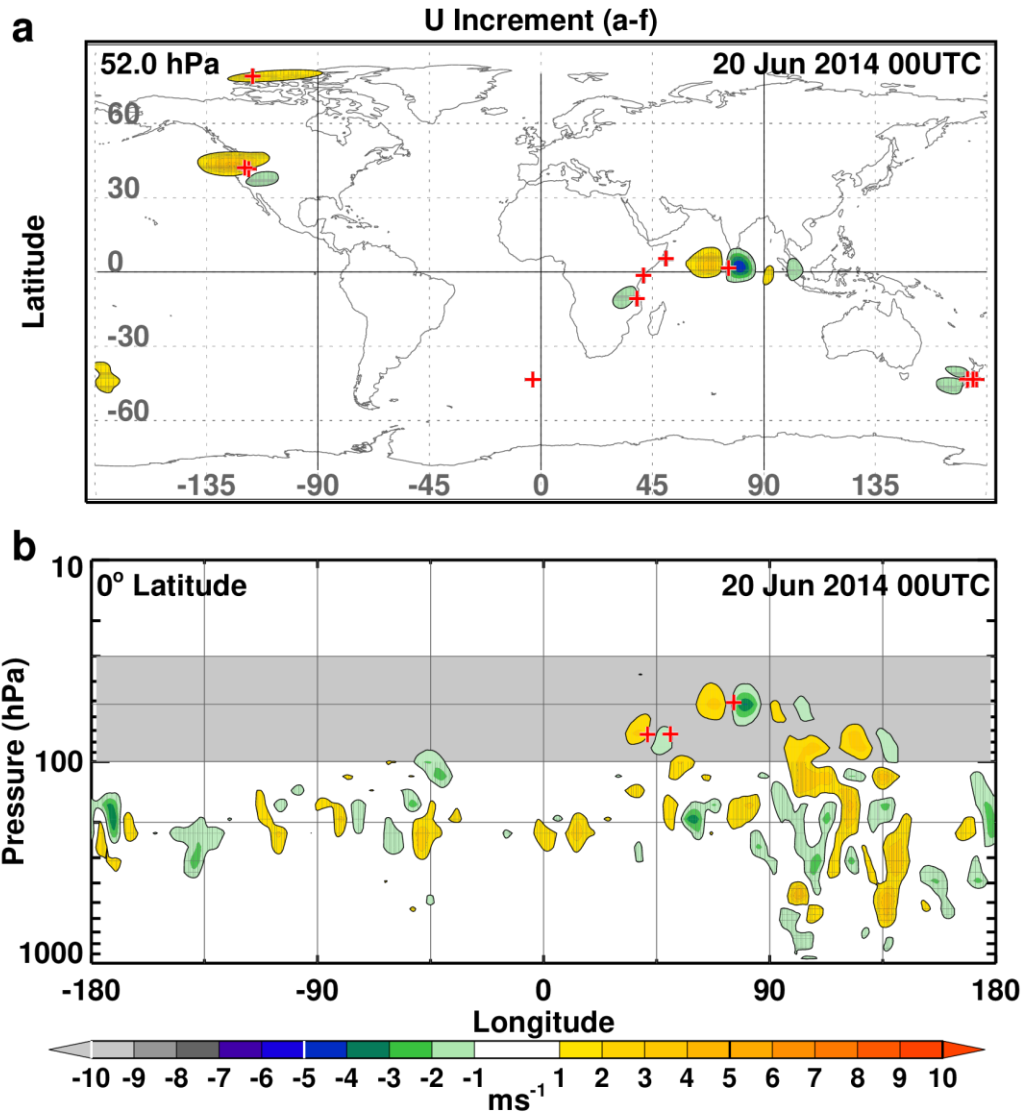


**Figure 3:** Assimilation zonal wind increment difference fields (see text) as a function of a) latitude and longitude at 52 hPa and b) longitude and pressure for 20 June 2014 00 UTC at 0° Latitude. The contour intervals are  $1 \text{ ms}^{-1}$  with orange/red positive and green/blue negative. Red plus symbols denote the balloon locations. Gray shading in b) denotes the region from 100-30 hPa.



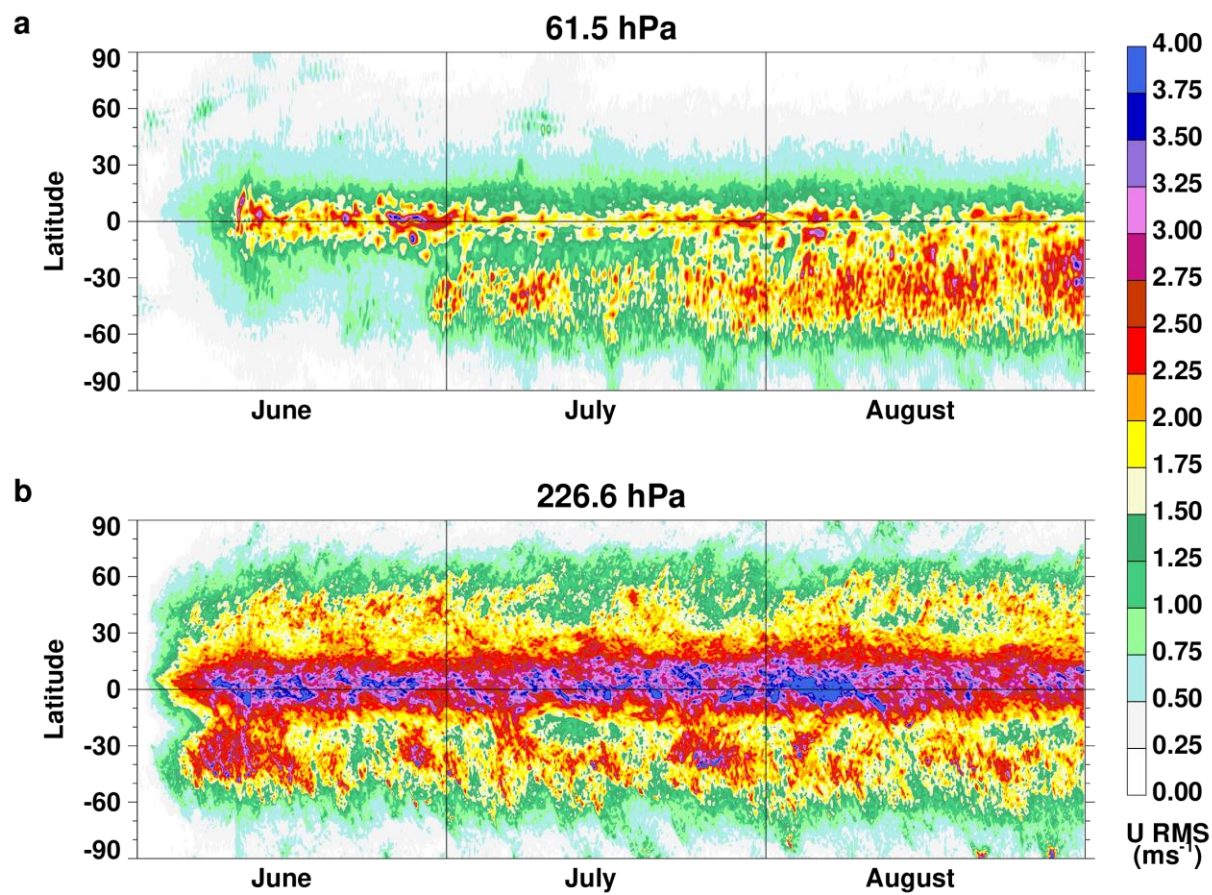


**Figure 4:** Zonal RMS differences (ms<sup>-1</sup>) between the Loon and control experiment zonal wind analysis fields at each three-hourly output time as a function of latitude and time at a) 61.5 hPa and b) 226.6 hPa).

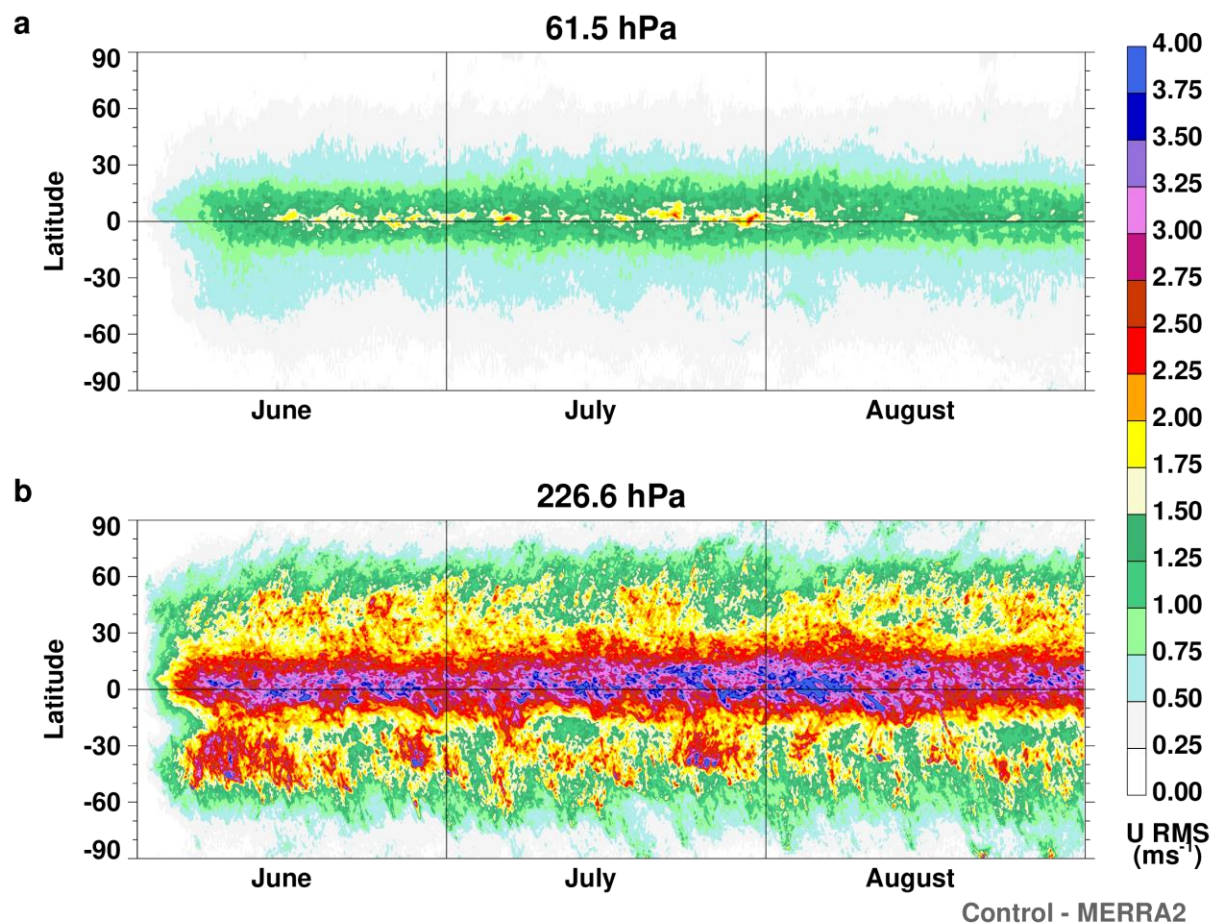


**Figure 5:** Same as Fig. 4 for the zonal RMS difference between the control experiments and MERRA-2.

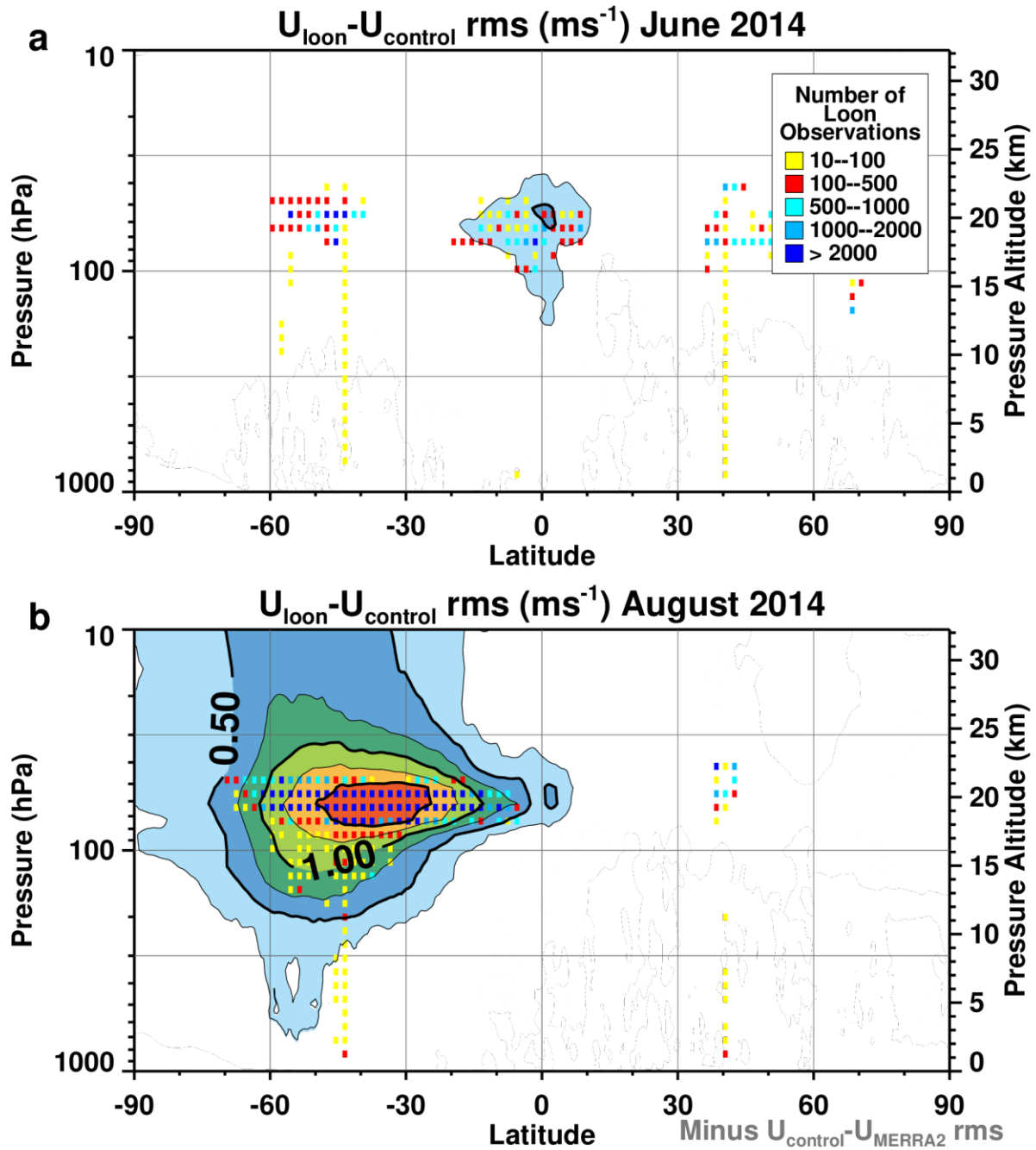
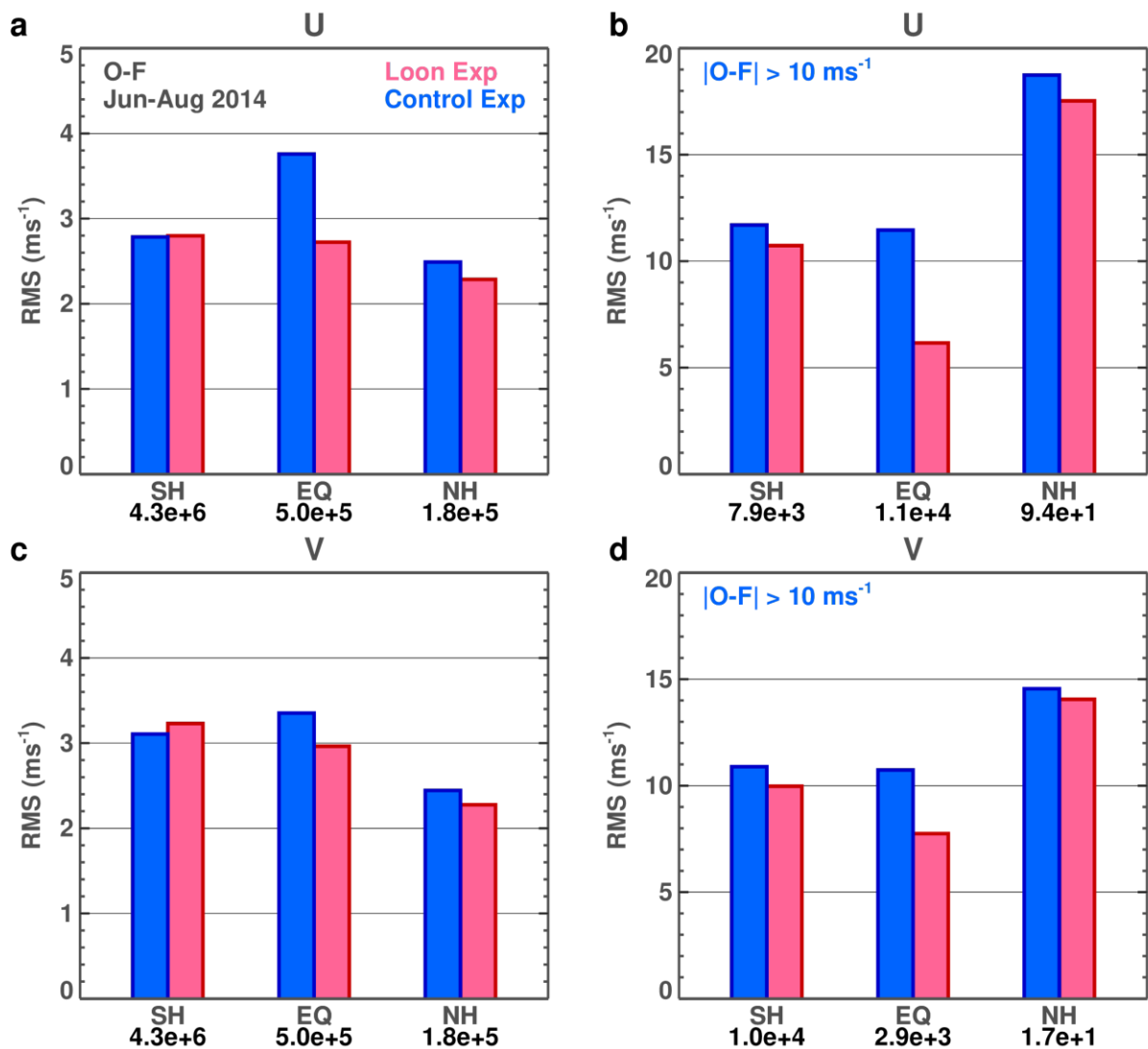


**Figure 6:** Zonal RMS differences ( $\text{ms}^{-1}$ ) between the Loon and control experiment zonal wind analysis fields as a function of latitude and pressure for a) June and b) August of 2014. The corresponding RMS difference between the control experiment and MERRA-2 has been subtracted to highlight the influence of the Loon balloons. The RMS with respect to longitude is calculated at each output time (8 times daily) and then averaged over the month. The contour interval is  $0.25 \text{ ms}^{-1}$ . The small squares are colored based on the number of Loon observations found within a  $1^\circ \times 500\text{m}$  (latitude by altitude) grid boxes as given by the insert in a). To clearly show the RMS contours only half of the grid boxes are plotted.

479  
480

481  
482



483  
484  
485  
486  
487  
488  
489  
490  
491

**Figure 7:** The root mean square (RMS) of the June-August 2014 Loon balloon winds observation minus forecast (O-F) for the Loon (Red) and the Control (Blue): a) zonal wind component, b) zonal wind component for Control O-F values greater than 10 ms<sup>-1</sup>, c) meridional wind component, and d) meridional zonal wind component for Control O-F values greater than 10 ms<sup>-1</sup>. Results in each panel are presented for three latitude ranges, SH, EQ, and NH, corresponding to, 90°S-20°S, 20°S-20°N, and 20°N-90°N. The numbers below each latitude range give the total number of Loon observations in that latitude range.



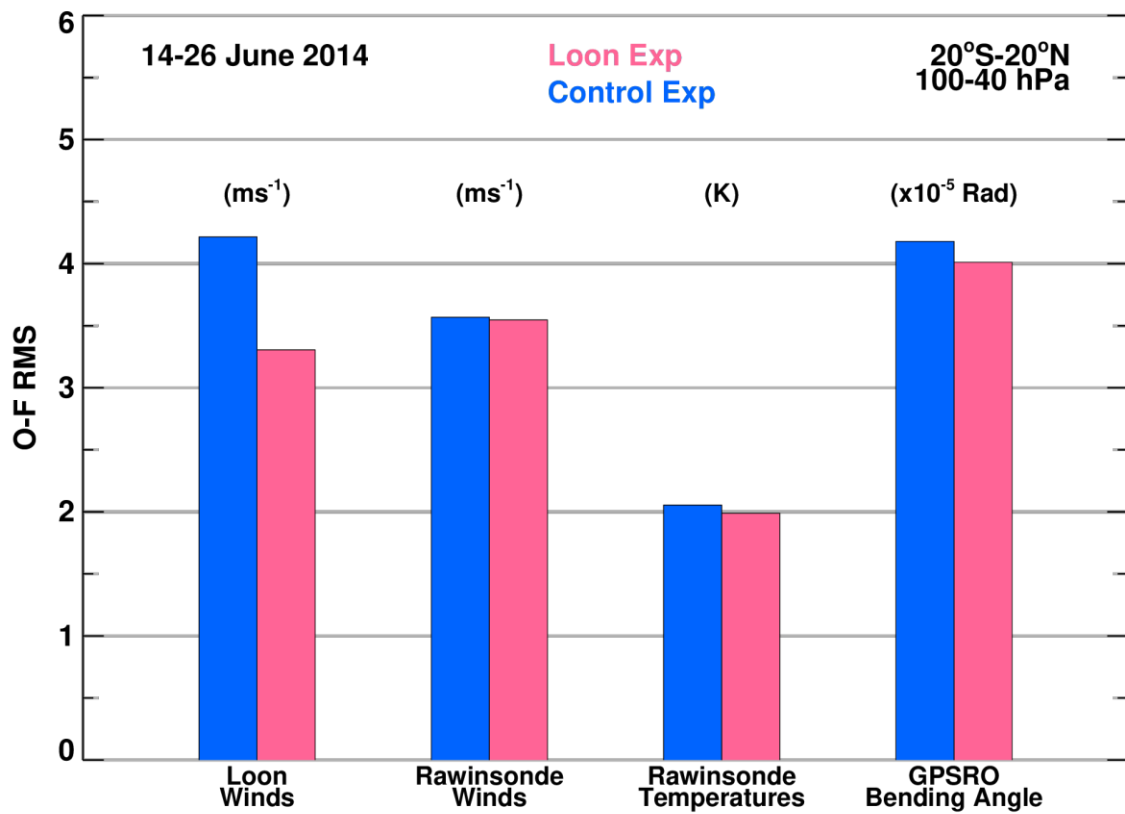


**Figure 8:** The root mean square (RMS) of the 14-26 June 2014 observation minus forecast (O-F) for the Loon experiment (Red) and the Control experiment (Blue) for the Loon zonal and meridional winds ( $\text{ms}^{-1}$ ), the radiosonde zonal and meridional winds ( $\text{ms}^{-1}$ ), the ransomed temperatures (K), and the GPSRO bending angle ( $\times 10^{-5}$  radians). The latitudes are from  $20^{\circ}\text{S}$  to  $20^{\circ}\text{N}$  and the pressure altitudes are from 100 to 40 hPa.

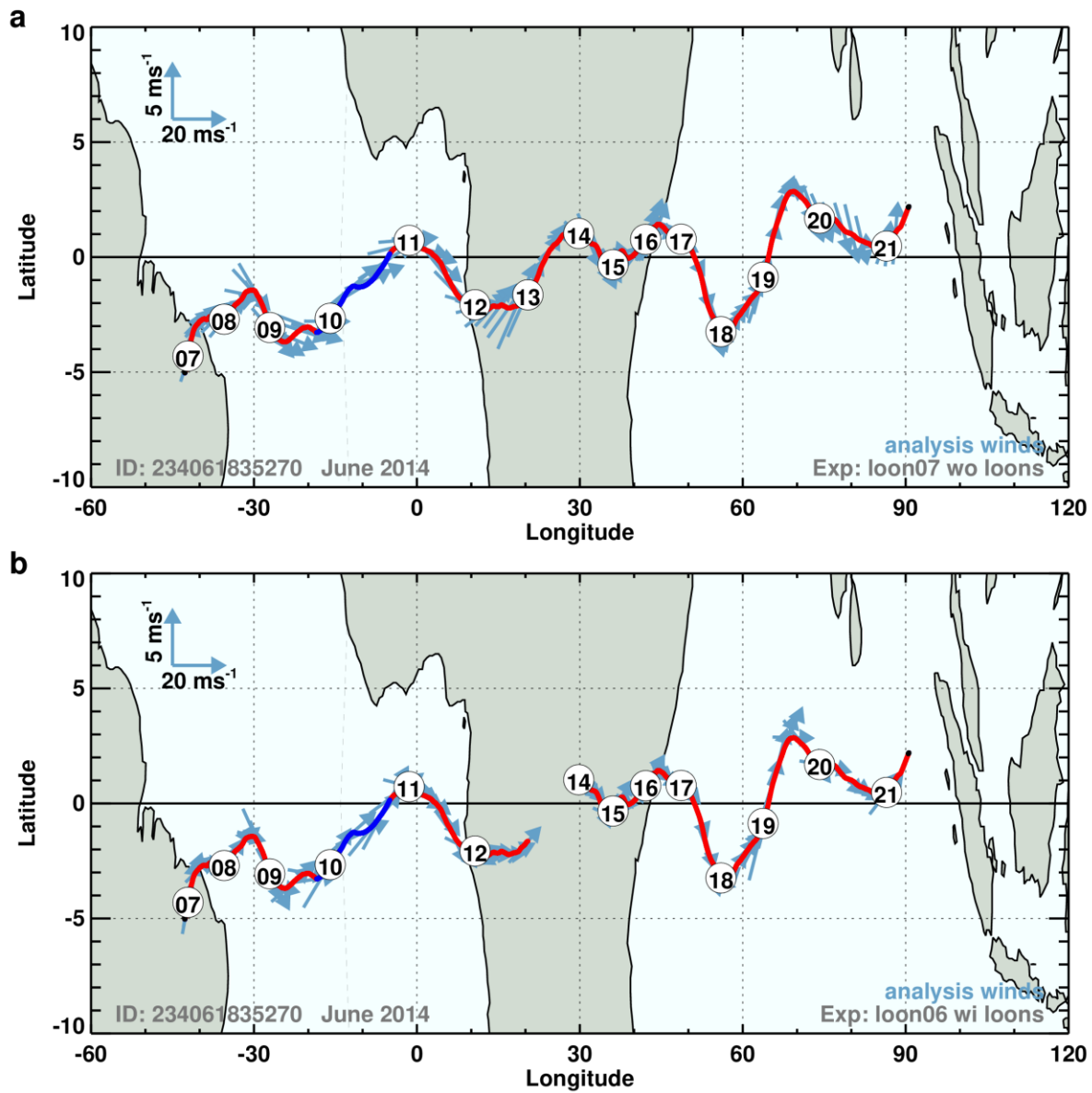


**Figure 9:** Loon balloon (234061835270) trajectory from 7-21 June 2014. Numbers shown in circles denote the 00 UTC Loon balloon location at that date in June. The red (blue) trajectory denotes pressure less than (greater than) 54 hPa. The arrows denote the hourly averaged wind speed and direction interpolated from the analysis to the balloon location for the a) Control and b) Loon experiments.



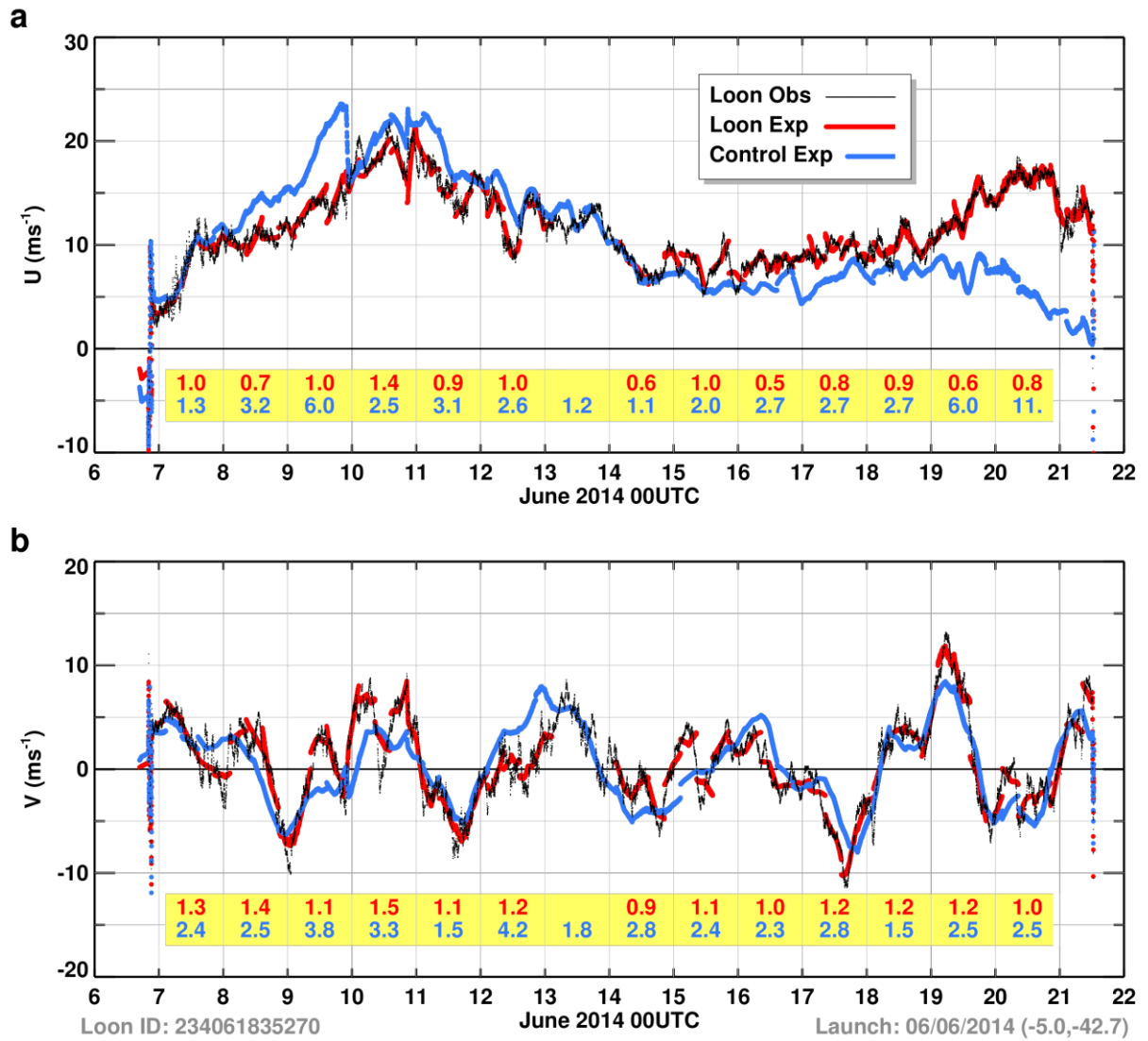


**Figure 10:** Example of the assimilation of one of the Loons over 7-21 June 2014 for a) the zonal wind component and b) the meridional wind component. Black points denote the balloon zonal wind observations. The blue points denote the control experiment analysis without the balloons and the red points denote the Loon experiment analysis. The daily RMS of the analysis minus the Loon values are given in the yellow strip below the corresponding day for the Loon (red) and the Control (blue).

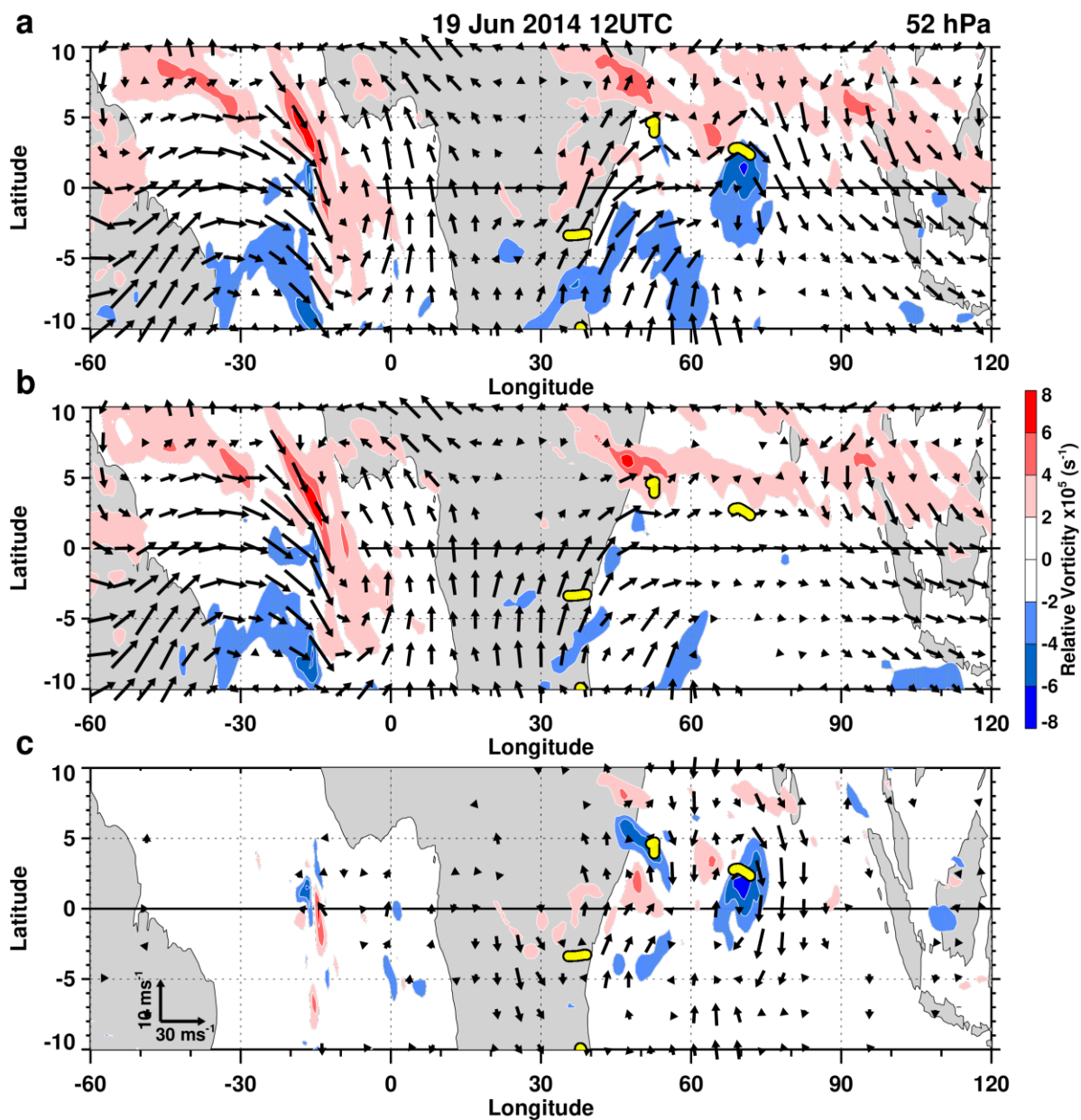


**Figure 11:** Example of the vector wind field (arrows) and relative vorticity (contours) at 52 hPa on 19 June 2014, 12 UTC for a) the Loon experiment, b) the Control experiment and c) the Loon minus the Control experiments. The yellow regions mark the location of the Loon balloon observations during the corresponding 6-hour assimilation data window.